THE OFFICIAL MAGAZINE OF THE OCEANOGRAPHY SOCIETY

Oceanography

CITATION

Christensen, K.H., Ø. Breivik, K.-F. Dagestad, J. Röhrs, and B. Ward. 2018. Short-term predictions of oceanic drift. *Oceanography* 31(3):59–67, https://doi.org/10.5670/oceanog.2018.310.

DOI

https://doi.org/10.5670/oceanog.2018.310

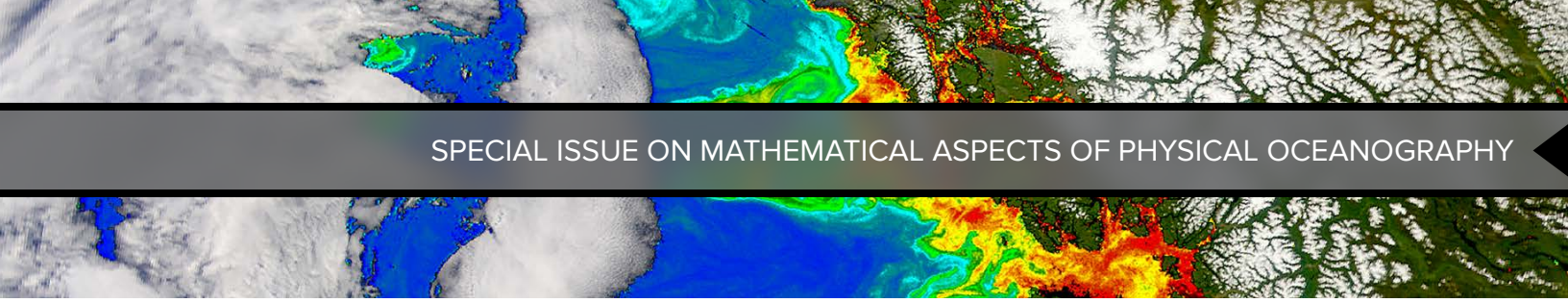

Short-Term Predictions of OCEANIC DRIFT

By Kai H. Christensen, Øyvind Breivik, Knut-Frode Dagestad, Johannes Röhrs, and Brian Ward

ABSTRACT. We discuss oceanic drift as relevant to applications in operational oceanography using examples from recent field experiments to highlight some of the challenges in modeling drift trajectories. Short-term predictions are important in time-critical operations, for example, for oil spill mitigation; hence, it is important that the transient response of the upper ocean to atmospheric forcing is modeled correctly. We emphasize the impact of surface waves and discuss the coupling between waves and mean flow in some detail. Because many objects of interest (e.g., person in water, oil spills) are in the wave zone, a better understanding of the details of the dynamics at the air-sea interface is needed. A clear separation of the forcing on such objects due to wind, waves, and ocean currents is needed in drift models, both to reduce dependence on empirical formulae and to make better use of drift data collected in field experiments.

INTRODUCTION

The need for short-term forecasts (hours to days) is common to many applications in operational oceanography, such as oil spill drift modeling or trajectory modeling for search-and-rescue support (Breivik et al., 2013; Dagestad et al., 2018). The output from several modeling systems must be combined—typically, numerical weather and wave and ocean circulation models—to provide forecasts from trajectory models of varying complexity (Davidson, 2009). For oceanic drift applications, the objects we need to consider are either (1) solid objects such as vessels (Eide et al., 2007), shipping containers (Breivik et al., 2012), or a person in water (Breivik and Allen, 2008), or (2) passive or buoyant tracers such as oil droplets (Jones et al., 2016), fish eggs (Röhrs et al., 2014; Strand et al., 2017), plastics (Kukulka et al., 2012; Van Sebille et al., 2012), or suspended radioactive material (Simonsen et al., 2017). For passive and buoyant tracers, we are primarily concerned with estimating the temporal and spatial distribution of the material, and possibly changes in the properties of the material with time due to its interaction with the environment. The intrinsic variability in ocean dynamics means that uncertainties can grow rapidly in time, but a lack of information about the objects of interest (e.g., last known position, shape and orientation, quantity and chemical composition of oils) can also lead to large errors. Most incidents happen with buoyant objects that are at or close to the surface, so that the direct and indirect influence of surface waves is important. Incidents typically also happen in the coastal zone, necessitating a detailed description of the bathymetry and the coastline. The problems we consider are inherently Lagrangian, as we follow the trajectories of specific objects in time. Ocean circulation models are Eulerian, and hence, we need to have specific models (or model components) for predicting drift trajectories (e.g., Van Sebille et al., 2018).

The main difference between Lagrangian and Eulerian velocities in the upper ocean is due to Stokes drift, which is the net forward motion in surface waves (Stokes, 1847). The Stokes drift has maximum value at the surface and decays rapidly with depth, contributing to the high vertical shear in drift velocities in the upper ocean. Stokes drift is also the manifestation of the mean momentum in the surface waves, and momentum fluxes between the waves and the mean flow also influence upper ocean dynamics and drift velocities (Longuet-Higgins, 1953). Surface waves also contribute to turbulent mixing in the upper ocean through various mechanisms such as wave breaking (Craig and Banner, 1994) and the induction of secondary flows such as Langmuir turbulence (e.g., Belcher et al., 2012). The details of these mechanisms have been intensely studied in recent years, but theoretical results are not yet properly backed up by observations (Esters et al., 2018), partly because of the difficulties in observing the upper ocean. It is not always clear how theoretical

understanding should be applied in practice, for instance, which one of several existing Langmuir turbulence mixing parameterizations to choose.

Our main aim in this paper is to provide a brief review of upper ocean drift on short temporal scales, and in particular the challenges involved in trying to model this drift. We are primarily interested in the vertical dynamical balances in deep water (i.e., the Ekman response), including the impact of surface waves. The smaller horizontal scales of submesoscale features (e.g., McWilliams, 2016) and nearshore circulation will therefore not be discussed here.

UPPER OCEAN MOMENTUM BUDGET

Two solutions that describe surface waves and that bear on our topic of interest were presented in the nineteenth century by Gerstner and by Stokes, respectively (for reviews see Craik, 2004; Henry, 2018). Gerstner waves are obtained as exact solutions of the Euler equations for free surface flow above infinite depth, and in these waves the water parcels move in closed orbits without any net motion. Gerstner waves possess mean vorticity, however, and cannot therefore be generated by conservative forces. In contrast, Stokes waves are irrotational, but with orbits that are not fully closed, and there is a net forward motion in the wave propagation direction. Today, wind-generated surface waves in the ocean are tacitly assumed to be Stokes waves, although we will briefly get back to this issue later on. The associated mean drift in waves, the Stokes drift $\boldsymbol{v}_S$, is an important quantity in coupled wave-ocean modeling systems. The Lagrangian velocity $\boldsymbol{v}_L$, with which objects are advected in the ocean, is thus taken to be the sum of Eulerian velocity $\boldsymbol{v}_E$ and the Stokes drift such that

$$\boldsymbol{v}_L = \boldsymbol{v}_E + \boldsymbol{v}_S. \quad (1)$$

An expression for Stokes drift for the case of a two-dimensional wave spectrum was derived by Kenyon (1969). Unfortunately, this expression is computationally expensive to evaluate from modeled wave spectra, and various approximations suitable for coupled modeling systems have therefore been developed (Breivik et al., 2014, 2016).

Wave growth and decay influence air-sea momentum fluxes, and Stokes drift can be used to evaluate the total wind- and wave-induced forcing of the mean ocean currents in numerical ocean circulation models (Jenkins, 1989). The underlying principle is simple and goes back to the pioneering work of Longuet-Higgins (1953) and the concept of virtual wave stress (Longuet-Higgins, 1969; see also Weber, 2001). The momentum flux $\boldsymbol{T}_o$ that drives the mean oceanic flow is a sum of a direct momentum flux from the atmosphere and a momentum flux from dissipating waves (e.g., through wave breaking). For example, assume that the total momentum flux from the atmosphere into both the waves and the oceanic mean flow is $\boldsymbol{T}_a$. If the waves are growing, $\boldsymbol{T}_o < \boldsymbol{T}_a$ because the momentum flux into the waves is larger than the momentum flux out of the waves and into the ocean (otherwise, the waves would not grow). Conversely, when the waves are decaying, $\boldsymbol{T}_o > \boldsymbol{T}_a$. The energy and the mean momentum in the waves are carried by the wave group velocity, so there is no reason for local balance, $\boldsymbol{T}_o = \boldsymbol{T}_a$. One obvious example is remotely forced swell that breaks in the nearshore and induces a mean flow there even in the absence of wind (e.g., Longuet-Higgins and Stewart, 1964). The Stokes transport $\boldsymbol{V}_S$ is the vertically integrated Stokes drift and represents the mean momentum in the surface waves (per unit density). The Stokes transport is easily calculated for small-amplitude waves (within the framework of linear theory) from modeled wave spectra, and formulations for wave-modulated ocean surface stress using Stokes transport are easily implemented in coupled wave-ocean modeling systems (Weber et al., 2006; Van den Bremer and Breivik, 2018). The average impact is typically fairly small (5%–10% increase or decrease in the stress, say), but can be substantial during rapidly changing weather conditions (e.g., Saetra et al., 2007). Model coupling efforts are in general based on theory for small-amplitude waves, and they are more challenging for large-amplitude waves because nonlinear effects become increasingly important (Constantin, 2006; Henry, 2006; Constantin and Strauss, 2010).

EKMAN RESPONSE TO WIND AND WAVES

Ekman (1905) formulated the classical solution to the problem of upper ocean response to wind in a rotating reference frame. Sudden onset of wind over a viscous ocean initially at rest leads to damped inertial oscillations with a period $T_f = 2\pi/f$ (where f is the Coriolis parameter or inertial frequency), superposed on a steady velocity at an angle to the wind, which is increasingly veering away from the wind and decaying rapidly with depth. The transient component can make offshore operations difficult due both to large amplitudes and to rapid rotation of the flow direction, and it is important to account for inertial oscillations when designing offshore structures (e.g., Bruserud et al., 2018). As a case in point, Figure 1 shows the drifter data collected during the Norwegian Clean Seas Association's oil-on-water exercise in June 2018. Two drifter triplets, each consisting of one MetOcean iSphere floating drifter (spherical shape, at the surface), one MetOcean self-locating datum marker buoy (iSLDMB or CODE, with a 1 m drogue centered at 0.7 m depth), and one MetOcean Surface Velocity Program (SVP) drifting buoy (with a 6 m drogue centered at 15 m depth), were deployed near the Frigg Field in the northern North Sea. Figure 1a shows the actual drifter trajectories over two inertial periods (2 × 13.8 h), while Figure 1b shows the trajectories obtained with the average displacement of one of the SVPs removed (the other SVP unfortunately lost its drogue soon after deployment). All of the drifters display the anticyclonic motion typical of inertial oscillations, and

the difference in the trajectories relative to the SVP exemplifies increased veering and decay with depth. The example should be interpreted with some caution, however, because the spherical drifters are subject to some wind drag and are advected by the Stokes drift (Röhrs et al., 2012), neither of which are accounted for in Ekman's analysis. It should also be noted that Ekman's solution is based on assuming a constant eddy viscosity, whereas in practice it varies with depth. Solutions to the Ekman problem with depth-dependent eddy viscosity are more realistic (e.g., Cronin and Kessler, 2009; Cronin and Tozuka, 2016), and regional differences in observed drift may be explained at least partially by regional differences in stratification and vertical variation in turbulence levels (Röhrs and Christensen, 2015).

The point here is that inertial oscillations are ubiquitous and can have large amplitudes, and it is vitally important that operational ocean circulation models accurately reproduce their dynamics to provide useful short-term forecasts. Small errors in the modeled phase of these oscillations may lead to large errors in modeled drift trajectories. On short timescales, $T < T_f$, the correlation between the local wind and observed drift is very low, but the correlation increases on timescales sufficiently long so that inertial oscillations can be averaged out (Röhrs and Christensen, 2015, see also Figure 3). Hence, we have a paradoxical situation in which producing an accurate long-term forecast can be less challenging than producing an accurate short-term forecast.

When stratification is taken into account, it is more accurate to use the term "near-inertial waves" (e.g., Alford et al., 2016) rather than "inertial oscillations." The frequency of near-inertial waves depends on both f and the buoyancy frequency N; hence, the ocean response to the atmospheric forcing produces a wider spectrum close to f that depends on the stratification. The near-inertial waves carry momentum and energy from the surface and downward, and may contribute to turbulent mixing at the base of the mixed layer if the velocity shear is sufficiently large. We will not go into detail here, but important challenges obviously include correctly modeling near-inertial wave generation and decay, and the influence of topography in shallow areas and close to the coast (e.g., Kim et al., 2015; Chen et al., 2015). It is also worth noting that including the local horizontal component of Earth's rotation in the governing equations allows for a wider range of near-inertial wave frequencies, including sub-inertial frequencies smaller than f (Shrira and Forget, 2015). The upper ocean response is made even more complex because the inertial oscillations or near-inertial waves may decay more slowly than the timescale of variations in the wind forcing. The observed oscillations can then be viewed as a superposition of oscillations from several wind events (e.g., Pollard and Millard, 1970; Chen et al., 2015). The amplitudes of the oscillations strongly depend on the nature of the changes in the forcing, for example, whether the local wind vector rotates cyclonically or anticyclonically, with anticyclonic rotation at a rate close to the inertial frequency producing the largest amplitudes (e.g., Röhrs and Christensen, 2015; Chen et al., 2015; Spencer et al., 2016). This property suggests that the wind history may provide useful information for modelers. Investigating the wind history (or forecast), more specifically the amplitude of the wind component that is in resonance with the inertial oscillations, may help us determine whether or not inertial oscillations are likely to be generated. Such information can potentially be useful for providing error estimates in model results. For an example, see Figure 2.

Mean flow equations that include surface wave effects tailored for numerical

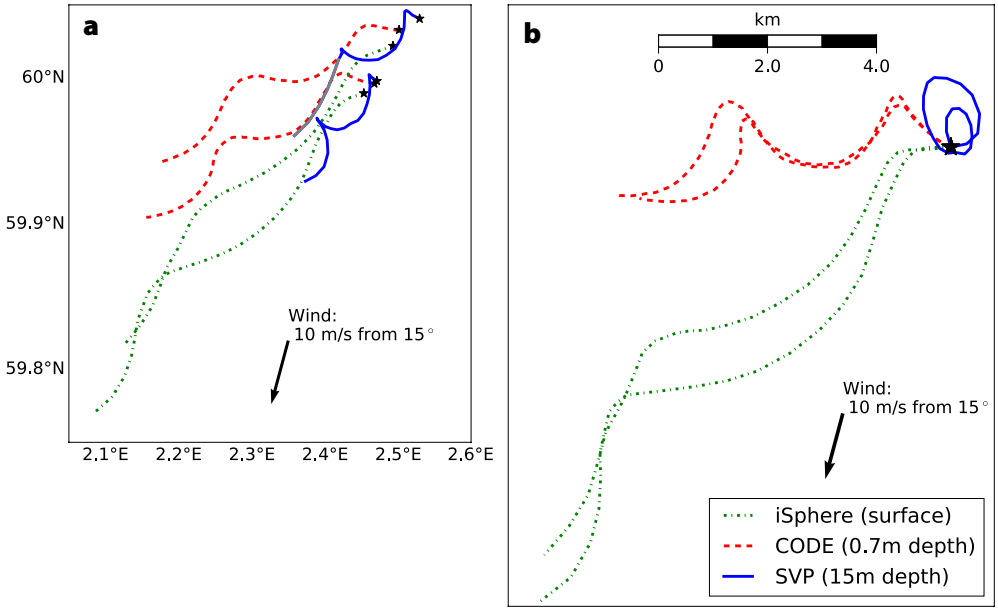

FIGURE 1. Trajectories from three different types of drifters as observed during the Norwegian Clean Seas Association's oil-on-water exercise in June 2018: iSphere (green dash-dotted line, 0 m depth), CODE drifters (red dashed line, 0.7 m depth), and SVP drifters (blue solid line, 15 m depth). One of the SVP drifters lost its drogue, after which the line is gray. The trajectories are plotted for two full inertial periods totaling 27.6 hours. Panel (a) shows the actual trajectories, while panel (b) shows the trajectories with the average displacement of one of the SVPs removed and using the same initial position for all units.

solution techniques are typically derived using semi-Lagrangian (e.g., Jenkins, 1989; Ardhuin et al., 2008) or Eulerian frameworks (e.g., McWilliams and Restrepo, 1999). For open ocean conditions, the most relevant terms include an addition to the Coriolis force (see below) and a vortex-force that generates Langmuir turbulence. The latter is characterized by small spatial and temporal scales that should be parameterized as part of a model's turbulence mixing scheme. Ursell was the first to investigate the influence of Earth's rotation on ocean surface waves (see Ursell and Deacon, 1950). Finding that the water parcels in this case move in closed orbits, he postulated that Stokes waves, under the influence of rotation, will within a short period of time (about a quarter of an inertial period) develop into Gerstner-*like* waves with no net mass transport. Pollard (1970) confirmed his results by obtaining an exact solution to the governing Lagrangian equations of motion on an *f*-plane. Later, Constantin and Monismith (2017) extended Pollard's analysis to include the effect of mean currents, which allows for a second wave mode close to the inertial frequency. Further extensions for Gerstner-like solutions in equatorial regions, where f is zero but the β-plane approximation applies, have been derived by Constantin (2012) and Henry (2016).

The impact on the mean Eulerian flow was neatly summed up by Hasselmann (1970), who showed that in a rotating ocean with waves, the Eulerian mean flow is subject to a body force per unit density $\boldsymbol{F}_f = -f\boldsymbol{k} \times \boldsymbol{v}_S$, which is referred to as the Coriolis-Stokes force. In an inviscid and homogeneous ocean, the Eulerian mean flow develops in such a way that the Lagrangian mean flow describes an undamped inertial oscillation with no net mass transport. The Coriolis-Stokes force is perhaps the least disputed wave-mean flow interaction term in ocean models, and is an important part of coupled modeling systems. Modeling studies have shown that the Coriolis-Stokes force can significantly influence the Ekman response (e.g., Polton et al., 2005). It is nevertheless challenging to find direct evidence of the influence of the Coriolis-Stokes force. Röhrs and Christensen (2015) used rotary spectrum analysis (Gonella, 1972) to investigate the correlation between local winds and observed drift. Substituting Stokes drift for the local wind provides some indication that the Coriolis-Stokes force does impact upper ocean drift velocities (Figure 4).

There is also strong feedback between the atmospheric boundary layer and the surface wave field. When waves grow, the roughness increases and the wind field above the ocean surface becomes more turbulent (Janssen, 1989, 1991) and acts as a drag on the atmosphere. This feeds back to the wave field through its impact on the evolution of the pressure field. This coupling is direct (i.e., mechanical) and therefore affects the wind field and the wave field on timescales of hours to days. The impact of the wave-ocean coupling on the full atmosphere-ocean system is more tenuous as it is a second-order thermodynamic feedback mechanism (Cavaleri et al., 2018), while the main impact (mixing the upper ocean) is achieved to leading order by mixing schemes with no

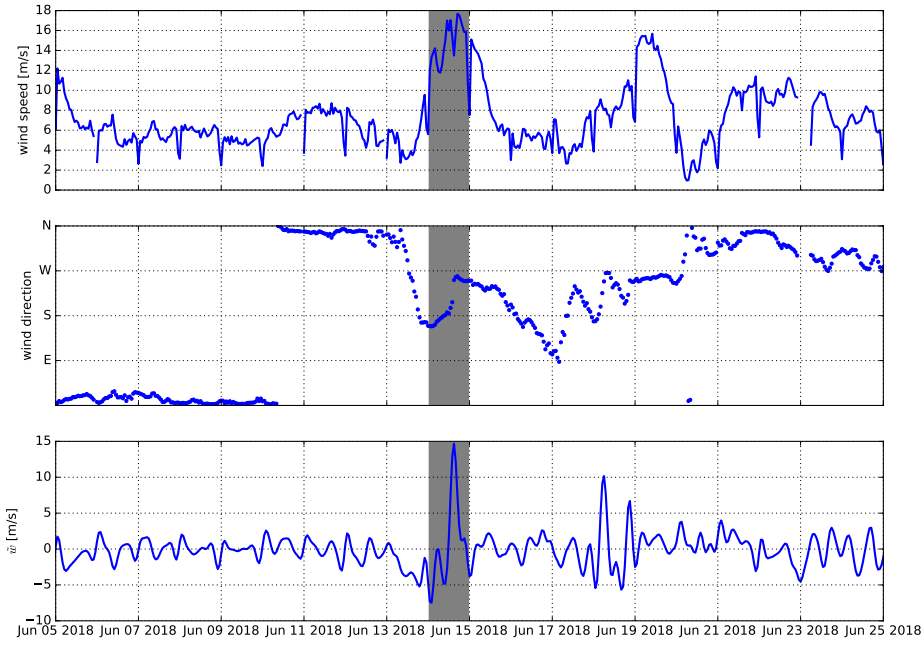

FIGURE 2. Wind speed and direction measured at the Heimdal offshore platform in the North Sea. Gray shading indicates a period with rapidly changing wind in resonance with inertial oscillations. The lower panel shows a filtered wind velocity that isolates the component of the wind close to the inertial frequency (convolution with a complex Morlet wavelet of length equal to $2T_f$).

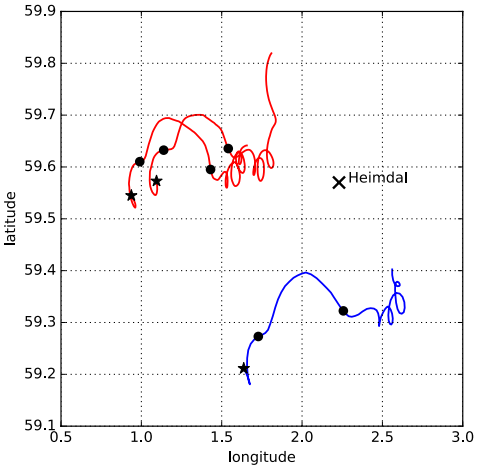

FIGURE 3. Location of the Heimdal offshore platform in relation to drifter trajectories. Drifter trajectories are shown in red for CODE drifters (0.7 m depth) and blue for the SVP drifter (15 m depth), with initial positions marked by stars. The drifters advance from southwest to northeast, and the parts of the trajectories marked with black dots correspond to the gray shaded time period in Figure 2. As is evident from the motion following this period, the resonant changes in the wind resulted in inertial oscillations.

wave effects included. However, as shown by Mogensen et al. (2017), upper ocean mixing can have a quite rapid effect in the case of tropical cyclones, where such enhanced mixing leads to Ekman pumping; thus, it is important to include wave-induced mixing in order to get the mixing right for the longer timescales (seasonal to climate).

UPPER OCEAN MIXING

The mixed layer of the ocean is typically turbulent because it is subject to the action of air-sea energy, momentum, and buoyancy fluxes (e.g., Esters et al., 2018). Wave breaking is an additional generation mechanism, along with Langmuir turbulence (Belcher et al., 2012), internal waves (Wain et al., 2015), and double diffusion (Walesby et al., 2015). Upper ocean turbulence is quantified by measuring the dissipation rate of turbulent kinetic energy. The processes controlling momentum transfer, gas exchange, and heat transfer are dominant at the air-sea interface. However, data from the upper few meters of the ocean are scarce, due to the complexity of collecting measurements in the surface wave field (i.e., $O(1) \times H_s$, where H_s is the significant wave height). Nonetheless, specialized technologies can overcome this challenge, for example, the Air-Sea Interaction Profiler (ASIP; Ward et al., 2014). ASIP is an autonomous profiling instrument that can cycle through the mixed layer at a typical rate of three to four profiles per hour. The sensor payload includes microstructure probes (shear, thermistor, conductivity) and accurate temperature and conductivity, pressure, and motion sensors. Dissipation is calculated using the shear probe data, which requires obtaining a power spectral density estimate for every 0.5 m, corresponding to 1,000 data points (Ward et al., 2014).

Measurements from this platform have demonstrated how rapid changes in atmospheric forcing can lead to dramatic changes in upper ocean turbulence. Figure 5 presents an example of dissipation data from ASIP during a deployment in the North Atlantic (Sutherland et al., 2013). From the start of the data set (approximately 15:00 local time) until 21:00, the wind speed is >10 m s^{-1} and the turbulence extends to about 20 m depth, which is quantified using estimates of mixing layer depth (XLD). The wind speed suddenly diminishes when a low pressure system passes, and there is an almost immediate response in the upper ocean mixing, with XLD shoaling to <10 m. At about 05:00, the center of the system moves past ASIP and the wind speed increases from 4 m s^{-1} to 17 m s^{-1}, causing a corresponding rapid deepening of the mixing layer depth. Throughout this period, the significant wave height remained mostly constant at approximately 2.5 m, indicating that wind-induced shear and breaking waves were the dominant turbulence-producing mechanisms.

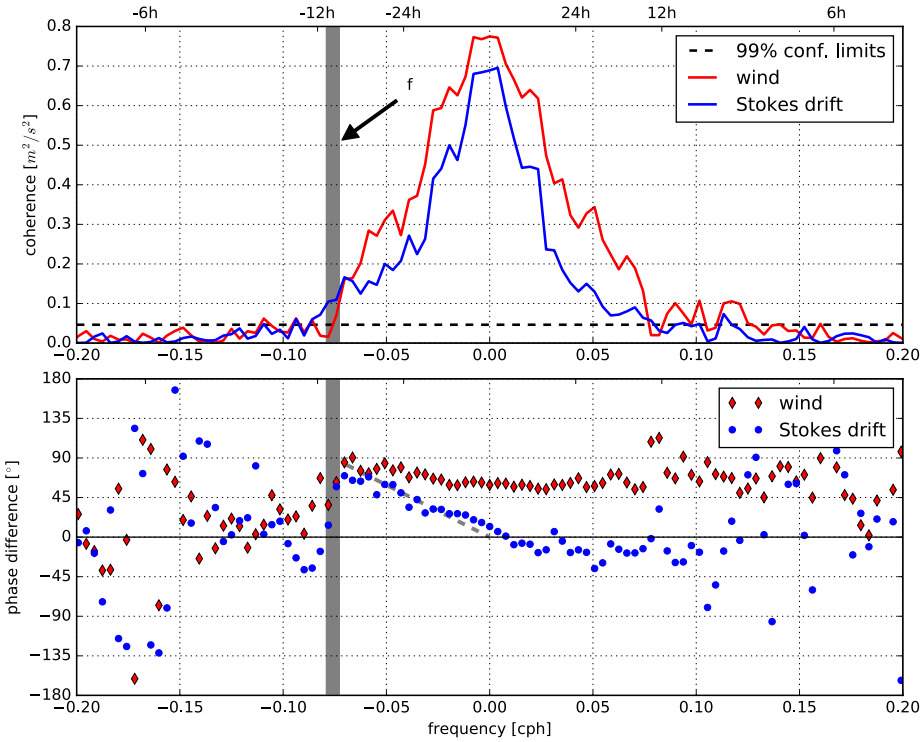

FIGURE 4. Coherence and phase difference between wind and drifter velocities (red) and between Stokes drift and drifter velocities (blue). The coherence spectra are based on rotary cross spectra between iSphere drifters (0 m depth) in the Norwegian Sea and wind and Stokes drift data from the NORA10 reanalysis (Reistad et al., 2011). The phase spectra show the angle or phase difference for coherent motions between drifter velocities and the wind/Stokes drift. Negative frequencies represent anticyclonic motions, with the ranges of the inertial frequencies at the drifter locations shaded in gray. Low-frequency cyclonic motion (positive frequencies) indicate simple advection by the Stokes drift (close to zero phase difference). For the anticyclonic motion, however, the phase difference steadily increases between the drift and the Stokes drift, and close to the inertial frequency the phase difference becomes similar to the veering typically associated with the classical Ekman response to the wind, indicating a more indirect influence of the Stokes drift possibly related to the Coriolis-Stokes force. Note that there is no coherence for superinertial frequencies, which means that there is seldom a one-to-one correspondence between the local forcing and the drifter motion on short times scales (Röhrs and Christensen, 2015).

From a modeling perspective, such observations clearly demonstrate that atmospheric forcing data with high temporal resolution is needed, and that ideally a fully coupled model system including the atmosphere, waves, and ocean should be used. Turbulent mixing by waves is typically introduced in two ways: (1) injection of turbulence kinetic energy at the surface due to breaking waves (Gemmrich et al., 1994; Craig and Banner, 1994), and (2) Langmuir turbulence. For instance, a number of available modifications to the so-called *K*-profile parameterizations (KPP, Large et al., 1994) of upper ocean turbulence

attempt to incorporate a measure of Langmuir turbulence production (see McWilliams and Sullivan, 2000; Smyth et al., 2002; M. Li et al., 2005; Harcourt and D'Asaro, 2008; Takaya et al., 2010; van Roekel et al., 2012). These are all based on extensions of the KPP where the turbulent Langmuir number, defined as $La_t = (u_* / v_{S0})^{½}$, with u_* the water-side friction velocity and v_{S0} the surface value of the Stokes drift, is raised to some negative power, and thus a measure of the sea state enters the production term (Belcher et al., 2012, noted that the square of La_t is really the ratio between the Stokes production and the shear production terms in the turbulence kinetic energy equation). Although this increases the mixing in places where models have biases today (such as the extra-tropics), it is a somewhat crude approach that only allows mixing to be increased, even when it is already too strong. Second moment turbulence closure schemes in the vein of Mellor and Yamada (1982) have been extended to incorporate Langmuir turbulence in a more direct fashion through a Stokes shear term (Janssen, 2012, Noh et al., 2016) or directly through introduction of the Craik-Leibovich vortex force (Harcourt 2013, 2015) in the turbulence closure. The impact of Langmuir turbulence on the mixed layer has recently been investigated using global coupled models of the ocean and the atmosphere (Fan and Griffies, 2014; Q. Li et al., 2016, 2017). The results suggest that the impact is largest in the wave-rich extra-tropics, where the sea surface temperature may change sufficiently to affect the atmospheric deep convection (Sheldon and Czaja, 2014).

DRIFT MODELING

Some ocean circulation models (e.g., Regional Ocean Modeling System [ROMS], Shchepetkin and McWilliams, 2005; Nucleus for European Modelling of the Ocean [NEMO], Madec et al., 2016) provide the possibility of computing the drift of passive tracers or particles along with the calculation of the geophysical fields. This is known as "online trajectory computations." The most common practice, however, is to use a separate trajectory model that takes the output from one or more Eulerian models as input for the drift calculations. Whereas such "offline trajectory computations" may also use a Eulerian grid for the computations (e.g., of concentration fields), a Lagrangian approach is by far the most common, where the objects or materials are represented by a number of discrete elements where the location is one of possibly many properties to be updated during the calculations (see Dagestad et al., 2018, for an overview). Although online trajectory computations avoid the need for a separate model, the offline Lagrangian models provide several important advantages. For drift modeling in support of emergency response (e.g., oil spills or search and rescue), calculation time is a critical factor, and results must be available within minutes or a few hours. Initiating a full three-dimensional ocean circulation model is then normally not feasible, and would also be a waste of resources. Another advantage of offline calculations is the possibility of combining input from several different Eulerian models, for instance, in the case of nested systems, taking advantage of increased resolution near the coastline. While ocean currents are obviously important, most of the objects or substances of interest are situated close to or at the ocean surface, where the impact of wind and waves might be at least as important as an ocean current. Thus, generally, a Lagrangian trajectory model would need to include input from an ocean model, a wave model, and an atmospheric model. For substances and small objects that are fully submerged (or for passive tracers), modeled vertical diffusivities are also important. As the horizontal velocity has a large shear in the upper ocean, vertical mixing has an important indirect impact on horizontal drift. This is well illustrated by the common observation of elongation of oil slicks in the wind direction, where oil that stays at the surface moves fastest in the downwind direction while oil that has been entrained and then resurfaced lags behind (Elliott et al., 1986; Jones et al., 2016). Note that such elongation is independent of Langmuir circulation, which may also lead to "banding" of oil or other surfactants along the wind direction.

It is normally assumed that drift trajectories follow the vector sum of the ambient ocean current and the Stokes drift at the given depth, adding a wind drag or wind drift factor as a percentage of the wind speed, for objects that are partially in air. For two examples of the relative importance of the advective terms and the wind forcing, see Figure 6. For floating objects that are not fully submerged,

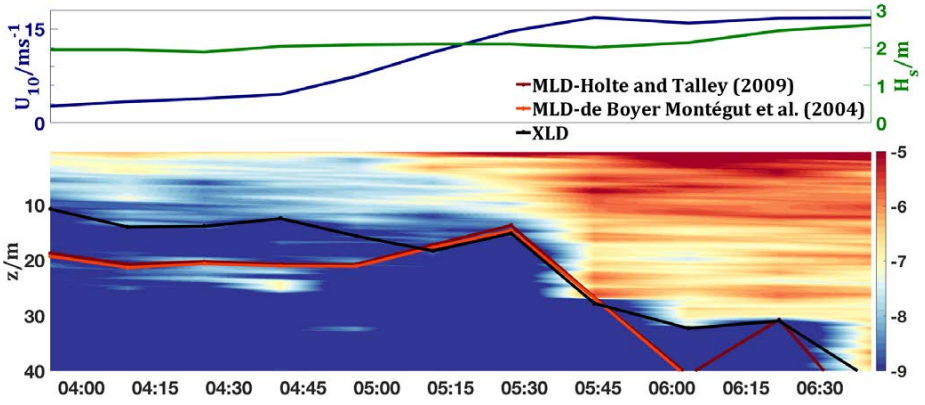

FIGURE 5. Data collected during a deployment of the Air-Sea Interaction Profiler (ASIP) in the North Atlantic on July 3, 2011. The upper panel shows the wind speed and significant wave height. The lower panel plots the dissipation rate (log scale) as well as estimates of the mixing layer depth (XLD) and mixed layer depth (MLD) using the two definitions of de Boyer Montegut et al. (2004) and Holte and Talley (2009), respectively.

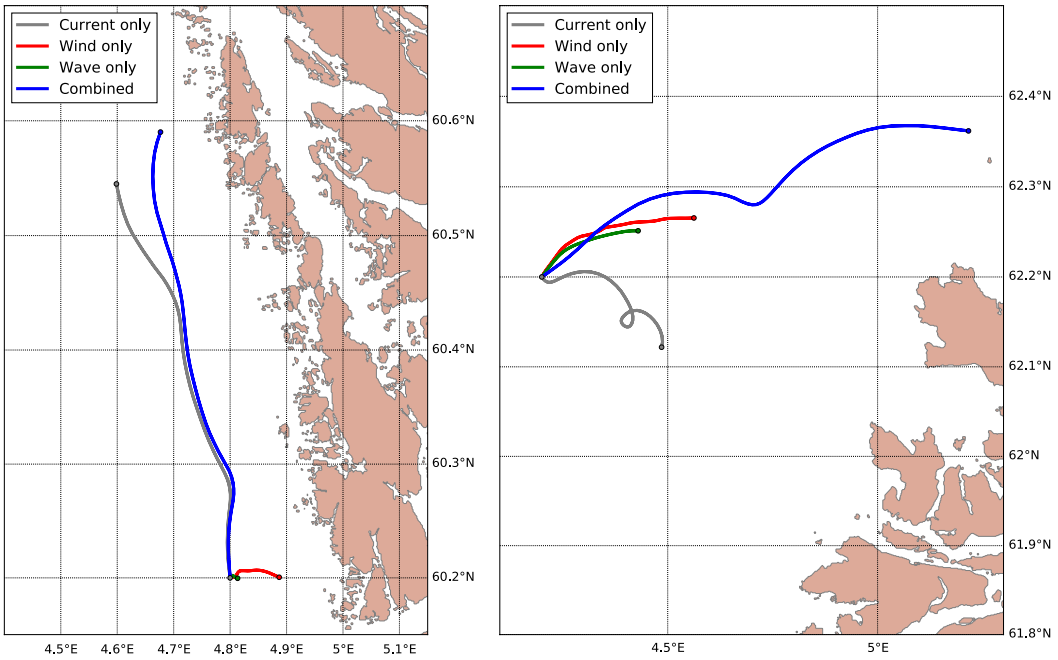

FIGURE 6. Simulated trajectories outside the Norwegian coast illustrating the relative importance of wind, waves, and currents for an object or substance at the ocean surface over 24 hours. For the example on the left (August 3, 2018), the wind is weak (around 3 m s^{-1}), and the object is located within a strong coastal current. For the example on the right (August 18, 2018), the wind is strong (around 12 m s^{-1}), and the object is located outside of the coastal current. Gray lines: drift follows the surface current. Red lines: drift is 2% of the wind speed. Green lines: drift follows the surface Stokes drift from a wave model. The blue lines show simulated trajectories using the combined forcing. Note that this is not expected to be identical to the vector sum of the other cases.

wind drag can be the dominant factor. For instance, for a life raft or small sailboat, the wind-induced drift (leeway) may be as large as 7% of the wind speed. Typically, the Stokes drift is implicitly included in the wind drift factor (Breivik and Allen, 2008).

The field data used to obtain this factor for various objects seldom contain sufficient information to assess the separate roles of wind drag and advection by the Stokes drift, with the exception of a few cases (e.g., Röhrs et al., 2012). Even for objects and substances that do not extend above the surface (e.g., oil slicks), it is often necessary to add a wind drift factor. In practice, this addition mainly compensates for the large vertical shear very close to the surface (Laxague et al., 2018), which is normally not resolved by ocean models with layer thicknesses of the order of decimeters to meters. However, empirically derived wind drift factors will also include other factors that are not directly considered, for instance, the feedback of an oil slick on wave-induced drift (Christensen and Terrile, 2009), and the high-frequency tail of the wave spectrum is commonly left out when numerically calculating the Stokes drift (Jones et al., 2016). Horizontal diffusivity is typically introduced to obtain realistic spreading and uncertainty, often by adding random perturbations (random walk) at each time step in Lagrangian drift models. The numerical values to use for diffusivity present an open question, however, as diffusivity is not a property of the flow in general, but rather depends on which spatial and temporal scales are resolved by the input models.

CONCLUDING REMARKS

The accuracy of short-term forecasts of upper ocean drift velocities depends on many factors. We have discussed the importance of the upper ocean's transient response to wind and wave forcing. To improve the predictions of the mean ocean circulation, a sensible approach is to put efforts into coupled modeling systems, observing systems, and ocean data assimilation (Wilkin et al., 2017). Better parameterizations of upper ocean mixing, including wave effects, are also needed, and existing turbulence scaling does not reflect observational data (Esters et al., 2018). Some model developments are potentially interesting, such as moving toward nonhydrostatic equations and including the horizontal component of the Coriolis force, none of which are commonly implemented in operational systems. Emphasis should nevertheless be on the uppermost part of the ocean, since this is where we find the majority of objects relevant to operational oceanography. For drift models, it is important to keep the forcing from wind, waves, and ocean currents separate. A better understanding of how wind drag on floating objects depends on sea state is needed. Smaller objects are typically entirely within the wave zone on both sides of the air-water interface, and ideally we would like to have a more sound theoretical basis for the force balance on such objects, removing some of our dependence on empirical data such as drag coefficients that include both direct wind forcing and advection by Stokes drift.

REFERENCES

Alford, M.H., J.A. MacKinnon, H.L. Simmons, and J.D. Nash. 2016. Near-inertial internal gravity waves in the ocean. *Annual Review of Marine Science* 8:95–123, https://doi.org/10.1146/annurev-marine-010814-015746.

Ardhuin, F., N. Rascle, and K.A. Belibassakis. 2008. Explicit wave-averaged primitive equations using a generalized Lagrangian mean. *Ocean Modelling* 20:35–60, https://doi.org/10.1016/j.ocemod.2007.07.001.

Belcher, S.E., A.L.M. Grant, K.E. Hanley, B. Fox-Kemper, L. Van Roekel, P.P. Sullivan, W.G. Large, A. Brown, A. Hines, D. Calvert, and others. 2012. A global perspective on Langmuir turbulence in the ocean surface boundary layer. *Geophysical Research Letters* 39(18), https://doi.org/10.1029/2012GL052932.

Breivik, Ø., and A.A. Allen. 2008. An operational search and rescue model for the Norwegian Sea and the North Sea. *Journal of Marine Systems* 69(1–2):99–113, https://doi.org/10.1016/j.jmarsys.2007.02.010.

Breivik, Ø., A.A. Allen, C. Maisondieu, and M. Olagnon. 2013. Advances in search and rescue at sea. *Ocean Dynamics* 63(1):83–88, https://doi.org/10.1007/s10236-012-0581-1.

Breivik, Ø., A.A. Allen, M. Maisondieu, J.-C. Roth, and B. Forest. 2012. The leeway of shipping containers at different immersion levels. *Ocean Dynamics* 62:741–752, https://doi.org/10.1007/s10236-012-0522-z.

Breivik, Ø., J.-R. Bidlot, and P.A.E.M. Janssen. 2016. A Stokes drift approximation based on the Phillips spectrum. *Ocean Modelling* 100:49–56, https://doi.org/10.1016/j.ocemod.2016.01.005.

Breivik, Ø., P.A.E. Janssen, and J.-R. Bidlot. 2014. Approximate Stokes drift profiles in deep water. *Journal of Physical Oceanography* 44:2,433–2,445, https://doi.org/10.1175/JPO-D-14-00201.

Bruserud, K., S. Haver, and D. Myrhaug. 2018. Simulated wind-generated inertial oscillations compared to current measurements in the northern North Sea. *Ocean Dynamics* 68:645–661, https://doi.org/10.1007/s10236-018-1150-z.

Cavaleri, L., S. Abdalla, A. Benetazzo, L. Bertotti, J.-R. Bidot, Ø. Breivik, S. Carniel, R.E. Jensen, J. Portilla-Yandun, W.E. Rogers, and others. 2018. Wave modelling in coastal and inner seas. *Progress in Oceanography,* https://doi.org/10.1016/j.pocean.2018.03.010.

Chen, S., J.A. Polton, J. Hu, and J. Xing. 2015. Local inertial oscillations in the surface ocean generated by time-varying winds. *Ocean Dynamics* 65:1,633–1,641, https://doi.org/10.1007/s10236-015-0899-6.

Christensen, K.H., and E. Terrile. 2009. Drift and deformation of oil slicks due to surface waves. *Journal of Fluid Mechanics* 620:313–332, https://doi.org/10.1017/S0022112008004606.

Constantin, A. 2006. The trajectories of particles in Stokes waves. *Inventiones Mathematicae* 166:523–535, https://doi.org/10.1007/s00222-006-0002-5.

Constantin, A. 2012. An exact solution for equatorially trapped waves. *Journal of Geophysical Research* 117, C05029, https://doi.org/10.1029/2012JC007879.

Constantin, A., and S.G. Monismith. 2017. Gerstner waves in the presence of mean currents and rotation. *Journal of Fluid Mechanics* 820:511–528, https://doi.org/10.1017/jfm.2017.223.

Constantin, A., and W. Strauss. 2010. Pressure beneath a Stokes wave. *Communications on Pure and Applied Mathematics* 63:533–557, https://doi.org/10.1002/cpa.20299.

Craig, P.D., and M.L. Banner. 1994. Modeling wave-enhanced turbulence in the ocean surface layer. *Journal of Physical Oceanography* 24:2,546–2,559, https://doi.org/10.1175/1520-0485(1994)024<2546:MWETIT>2.0.CO;2.

Craik, A.D. 2004. The origins of water wave theory. *Annual Review of Fluid Mechanics* 36:1–28, https://doi.org/10.1146/annurev.fluid.36.050802.122118.

Cronin, M.F., and W.S. Kessler. 2009. Near-surface shear flow in the tropical Pacific cold tongue front. *Journal of Physical Oceanography* 39:1,200–1,215, https://doi.org/10.1175/2008JPO4064.1.

Cronin, M.F., and T. Tozuka. 2016. Steady state ocean response to wind forcing in extratropical frontal regions. *Scientific Reports* 6, 28842, https://doi.org/10.1038/srep28842.

Dagestad, K.-F., J. Röhrs, Ø. Breivik, and B. Aadlandsvik. 2018. OpenDrift v1.0: A generic framework for trajectory modeling. *Geoscientific Model Development* 11:1,405–1,420, https://doi.org/10.5194/gmd-11-1405-2018.

Davidson, F.J.M., A. Allen, G.B. Brassington, Ø. Breivik, P. Daniel, M. Kamachi, S. Sato, B. King, F. Lefevre, M. Sutton, and H. Kaneko. 2009. Applications of GODAE ocean current forecasts to search and rescue and ship routing. *Oceanography* 22(3):176–181, https://doi.org/10.5670/oceanog.2009.76.

de Boyer Montegut, C., G. Madec, A.S. Fischer, A. Lazar, and D. Ludicone. 2004. Mixed layer depth over the global ocean: An examination of profile data and a profile-based climatology. *Journal of Geophysical Research* 109, C12003, https://doi.org/10.1029/2004JC002378.

Eide, M.S., Ø. Endresen, Ø. Breivik, O.W. Brude, I.H. Ellingsen, K. Røang, J. Hauge, and P.O. Brett. 2007. Prevention of oil spill from shipping by modelling of dynamic risk. *Marine Pollution Bulletin* 54:1,619–1,633, https://doi.org/10.1016/j.marpolbul.2007.06.013.

Ekman, V.W. 1905. On the influence of the Earth's rotation on ocean currents. *Arkiv för matematik, astronomi och fysik* 2:1–52.

Elliott, A.J., N. Hurford, and C.J. Penn. 1986. Shear diffusion and the spread of oil in the surface layers of the North Sea. *Deutsche Hydrografische Zeitschrift* 39:113–137, https://doi.org/10.1007/BF02408134.

Esters, L., Ø. Breivik, S. Landwehr, G.S.A. ten Doeschate, K.H. Christensen, J.-R. Bidlot, and B. Ward. 2018. Turbulence scaling comparisons in the ocean surface boundary layer. *Journal of Geophysical Research* 123:2,172–2,191, https://doi.org/10.1002/2017JC013525.

Fan, Y., and S.M. Griffies. 2014. Impacts of parameterized Langmuir turbulence and non-breaking wave mixing in global climate simulations. *Journal of Climate* 27:4,752–4,775, https://doi.org/10.1175/JCLI-D-13-00583.1.

Gemmrich, J.R., T.D. Mudge, and V.D. Polonichko. 1994. On the energy input from wind to surface waves. *Journal of Physical Oceanography* 24:2,413–2,417, https://doi.org/10.1175/1520-0485(1994)024<2413:OTEIFW>2.0.CO;2.

Gonella, J. 1972. A rotary-component method for analysing meteorological and oceanographic vector time series. *Deep Sea Research and Oceanographic Abstracts* 19:833–846, https://doi.org/10.1016/0011-7471(72)90002-2.

Harcourt, R.R. 2013. A second-moment closure model of Langmuir turbulence. *Journal of Physical Oceanography* 43:673–697, https://doi.org/10.1175/JPO-D-12-0105.1.

Harcourt, R.R. 2015. An improved second-moment closure model of Langmuir turbulence. *Journal of Physical Oceanography* 45:84–103, https://doi.org/10.1175/JPO-D-14-0046.1.

Harcourt, R.R., and E.A. D'Asaro. 2008. Large-eddy simulation of Langmuir turbulence in pure wind seas. *Journal of Physical Oceanography* 38:1,542–1,562, https://doi.org/10.1175/2007JPO3842.1.

Hasselmann, K. 1970. Wave-driven inertial oscillations. *Geophysical Fluid Dynamics* 1:463–502, https://doi.org/10.1080/03091927009365783.

Henry, D. 2006. The trajectories of particles in deep-water Stokes waves. *International Mathematics Research Notices*, 23405, https://doi.org/10.1155/IMRN/2006/23405.

Henry, D. 2016. Equatorially trapped nonlinear water waves in a β-plane approximation with centripetal forces. *Journal of Fluid Mechanics* 804, R1, https://doi.org/10.1017/jfm.2016.544.

Henry, D. 2018. On three-dimensional Gerstner-like equatorial water waves. *Philosphical Transactions of the Royal Society A* 376, 20170088, https://doi.org/10.1098/rsta.2017.0088.

Holte, J., and L. Talley. 2009. A new algorithm for finding mixed layer depths with applications to Argo data and subantarctic mode water formation. *Journal of Atmospheric and Oceanic Technology* 26:1,920–1,939, https://doi.org/10.1175/2009JTECHO543.1.

Janssen, P.A.E.M. 1989. Wave-induced stress and the drag of air flow over sea waves. *Journal of Physical Oceanography* 19:745–754, https://doi.org/10.1175/1520-0485(1989)019<0745:WISATD>2.0.CO;2.

Janssen, P.A.E.M. 1991. Quasi-linear theory of wind-wave generation applied to wave forecasting. *Journal of Physical Oceanography* 21:1,631–1,642, https://doi.org/10.1175/1520-0485(1991)021<1631:QLTOWW>2.0.CO;2.

Janssen, P.A.E.M. 2012. Ocean wave effects on the daily cycle in SST. *Journal of Geophysical Research* 117(C11), https://doi.org/10.1029/2012JC007943.

Jenkins, A.D. 1989. The use of a wave prediction model for driving a near-surface current model. *Deutsche Hydrografische Zeitschrift* 42:133–149, https://doi.org/10.1007/BF02226291.

Jones, C., K.-F. Dagestad, Ø. Breivik, B. Holt, J. Röhrs, K.H. Christensen, M. Espeseth, C. Brekke, and S. Skrunes. 2016. Measurement and modeling of oil slick transport. *Journal of Geophysical Research* 121:7,759–7,775, https://doi.org/10.1002/2016JC012113.

Kenyon, K.E. 1969. Stokes drift for random gravity waves. *Journal of Geophysical Research* 74(28):6,991–6,994, https://doi.org/10.1029/JC074i028p06991.

Kim, S.Y., A.L. Kurapov, and P.M. Kosro. 2015. Influence of varying upper ocean stratification on coastal near-inertial currents. *Journal of Geophysical Research* 120:8,504–8,527, https://doi.org/10.1002/2015JC011153.

Kukulka, T., G. Proskurowski, S. Morét-Ferguson, D.W. Meyer, and K.L. Law. 2012. The effect of wind mixing on the vertical distribution of buoyant plastic debris. *Geophysical Research Letters* 39(7), https://doi.org/10.1029/2012GL051116.

Laxague, N.J.M., T.M. Özgökmen, B.K. Haus, G. Novelli, A. Shcherbina, P. Sutherland, C.M. Guigand, B. Lund, S. Mehta, M. Alday, and others. 2018. Observations of near-surface current shear help describe oceanic oil and plastic transport. *Geophysical Research Letters* 44:245–249, https://doi.org/10.1002/2017GL075891.

Large, W.G., J.C. McWilliams, and S.C. Doney. 1994. Oceanic vertical mixing: A review and a model with a nonlocal boundary layer parameterization. *Reviews of Geophysics* 32:363–403, https://doi.org/10.1029/94RG01872.

Li, M., C. Garrett, and E. Skyllingstad. 2005. A regime diagram for classifying turbulent large eddies in the upper ocean. *Deep Sea Research Part I* 52:259–278, https://doi.org/10.1016/j.dsr.2004.09.004.

Li, Q., B. Fox-Kemper, Ø. Breivik, and A. Webb. 2017. Statistical models of global Langmuir mixing. *Ocean Modelling* 113:95–114, https://doi.org/10.1016/j.ocemod.2017.03.016.

Li, Q., A. Webb, B. Fox-Kemper, A. Craig, A. Danabasoglu, W.G. Large, and M. Vertenstein. 2016. Langmuir mixing effects on global climate: WAVEWATCH III in CESM. *Ocean Modelling* 103:145–160, https://doi.org/10.1016/j.ocemod.2015.07.020.

Longuet-Higgins, M.S. 1953. Mass transport in water waves. *Philosphical Transactions of the Royal Society A* 245:535–581, https://doi.org/10.1098/rsta.1953.0006.

Longuet-Higgins, M.S. 1969. A nonlinear mechanism for the generation of sea waves. *Proceedings of the Royal Society A* 311:371–389, https://doi.org/10.1098/rspa.1969.0123.

Longuet-Higgins, M.S., and R.W. Stewart. 1964. Radiation stresses in water waves: A physical discussion, with applications. *Deep Sea Research and Oceanographic Abstracts* 11:529–562, https://doi.org/10.1016/0011-7471(64)90001-4.

Madec, G., and the NEMO team. 2016. *NEMO Ocean Engine*. Note du Pôle de modélisation de l'Institut Pierre-Simon Laplace No. 27, France, 396 pp., https://www.nemo-ocean.eu/wp-content/uploads/NEMO_book.pdf.

McWilliams, J.C. 2016. Submesoscale currents in the ocean. *Proceedings of the Royal Society A* 472, 20160117, https://doi.org/10.1098/rspa.2016.0117.

McWilliams, J.C., and J.M. Restrepo. 1999. The wave-driven ocean circulation. *Journal of Physical Oceanography* 29:2,523–2,540, https://doi.org/10.1175/1520-0485(1999)029<2523:TWDOC>2.0.CO;2.

McWilliams, J.C., and P.P. Sullivan. 2000. Vertical mixing by Langmuir circulations. *Spill Science & Technology Bulletin* 6:225–237, https://doi.org/10.1016/S1353-2561(01)00041-X.

Mellor, G.L., and T. Yamada. 1982. Development of a turbulent closure model for geophysical fluid problems. *Reviews of Geophysics and Space Physics* 20:851–875, https://doi.org/10.1029/RG020i004p00851.

Mogensen, K.S., L. Magnusson, and J.-R. Bidlot. 2017. Tropical cyclone sensitivity to ocean coupling in the ECMWF coupled model. *Journal of Geophysical Research* 122:4,392–4,412, https://doi.org/10.1002/2017JC012753.

Noh, Y., H. Ok, E. Lee, T. Toyoda, and N. Hirose. 2016. Parameterization of Langmuir circulation in the ocean mixed layer model using LES and its application to the OGCM. *Journal of Physical Oceanography* 46:57–78, https://doi.org/10.1175/JPO-D-14-0137.1.

Pollard, R.T. 1970. Surface waves with rotation: An exact solution. *Journal of Geophysical Research* 75:5,895–5,898, https://doi.org/10.1029/JC075i030p05895.

Pollard, R.T., and R.C. Millard. 1970. Comparison between observed and simulated wind-generated inertial oscillations. *Deep Sea Research and Oceanographic Abstracts* 17:813–821, https://doi.org/10.1016/0011-7471(70)90043-4.

Polton, J.A., D.M. Lewis, and S.E. Belcher. 2005. The role of wave-induced Coriolis-Stokes forcing on the wind-driven mixed layer. *Journal of Physical Oceanography* 35:444–457, https://doi.org/10.1175/JPO2701.1.

Reistad, M., Ø. Breivik, H. Haakenstad, O.J. Aarnes. B.R. Furevik, and J.-R. Bidlot. 2011. A high-resolution hindcast of wind and waves for the North Sea, the Norwegian Sea, and the Barents Sea. *Journal of Geophysical Research* 116(C5), https://doi.org/10.1029/2010JC006402.

Röhrs, J., and K.H. Christensen. 2015. Drift in the uppermost part of the ocean. *Geophysical Research Letters* 42:10,349–10,356, https://doi.org/10.1002/2015GL066733.

Röhrs, J., K.H. Christensen, L.R. Hole, G. Broström, M. Drivdal, and S. Sundby. 2012. Observation-based evaluation of surface wave effects on currents and trajectory forecasts. *Ocean Dynamics* 62:1,519–1,533, https://doi.org/10.1007/s10236-012-0576-y.

Röhrs, J., K.H. Christensen, F. Vikebø, S. Sundby, Ø. Saetra, and G. Broström. 2014. Wave-induced transport and vertical mixing of pelagic eggs and larvae. *Limnology and Oceanography* 59:1,213–1,227, https://doi.org/10.4319/lo.2014.59.4.1213.

Saetra, Ø., J. Albretsen, and P.A. Janssen. 2007. Sea-state-dependent momentum fluxes for ocean modeling. *Journal of Physical Oceanography* 37:2,714–2,725, https://doi.org/10.1175/2007JPO3582.1.

Shchepetkin, A.F., and J.C. McWilliams. 2005. The regional oceanic modeling system (ROMS): A split-explicit, free-surface, topography-following-coordinate oceanic model. *Ocean Modelling* 9:347–404, https://doi.org/10.1016/j.ocemod.2004.08.002.

Sheldon, L., and A. Czaja. 2014. Seasonal and interannual variability of an index of deep atmospheric convection over western boundary currents. *Quarterly Journal of the Royal Meteorological Society* 140(678):22–30, https://doi.org/10.1002/qj.2103.

Shrira, V.I., and P. Forget. 2015. On the nature of near-inertial oscillations in the uppermost part of the ocean and a possible route toward HF radar probing of stratification. *Journal of Physical Oceanography* 45:2,660–2,678, https://doi.org/10.1175/JPO-D-14-0247.1.

Simonsen, M., Ø. Saetra, P.E. Isachsen, O.C. Lind, H.K. Skjerdal, B. Salbu, H.E. Heidal, and J.P. Gwynn. 2017. The impact of tidal and mesoscale eddy advection on the long term dispersion of ^{99}Tc from Sellafield. *Journal of Environmental Radioactivity* 177:100–112, https://doi.org/10.1016/j.jenvrad.2017.06.002.

Smyth, W.D., E.D. Skyllingstad, G.B. Crawford, and H. Wijesekera. 2002. Nonlocal fluxes and Stokes drift effects in the K-profile parameterization. *Ocean Dynamics* 52:104–115, https://doi.org/10.1007/s10236-002-0012-9.

Spencer, L.J., S.F. DiMarco, Z. Wang, J.J. Kuehl, and D.A. Brooks. 2016. Asymmetric oceanic response to a hurricane: Deep water observations during Hurricane Isaac. *Journal of Geophysical Research* 121:7,619–7,649, https://doi.org/10.1002/2015JC011560.

Stokes, G.G. 1847. On the theory of oscillatory waves. *Transactions of the Cambridge Philosophical Society* 8(441)197–229.

Strand, K.O., S. Sundby, J. Albretsen, and F.B. Vikebø. 2017. The Northeast Greenland shelf as a potential habitat for the Northeast Arctic cod. *Frontiers in Marine Science* 4:304, https://doi.org/10.3389/fmars.2017.00304.

Takaya, Y., J.-R. Bidlot, A. Beljaars, and P.A.E.M. Janssen. 2010. Refinements to a prognostic scheme of skin sea surface temperature. *Journal of Geophysical Research* 115(C6), https://doi.org/10.1029/2009JC005985.

Ursell, F., and G. Deacon. 1950. On the theoretical form of ocean swell on a rotating Earth. *Geophysical Journal International* 6:1–8, https://doi.org/10.1111/j.1365-246X.1950.tb02968.x.

Van den Bremer, T., and Ø. Breivik. 2018. Stokes drift. *Philosphical Transactions of the Royal Society A* 376, https://doi.org/10.1098/rsta.2017.0104.

Van Roekel, L.P., B. Fox-Kemper, P.P. Sullivan, P.E. Hamlington, and S.R. Haney. 2012. The form and orientation of Langmuir cells for misaligned winds and waves. *Journal of Geophysical Research* 117(C5), https://doi.org/10.1029/2011JC007516.

Van Sebille, E., M.H. England, and G. Froyland. 2012. Origin, dynamics and evolution of ocean garbage patches from observed surface drifters. *Environmental Research Letters* 7, 044040, https://doi.org/10.1088/1748-9326/7/4/044040.

Van Sebille, E., S.M. Griffies, R. Abernathy, T.P. Adams, P. Berloff, A. Biastoch, B. Blanke, E.P. Chassignet, Y. Cheng, C.J. Cotter, and others. 2018. Lagrangian ocean analysis: Fundamentals and practices. *Ocean Modelling* 121:49–75, https://doi.org/10.1016/j.ocemod.2017.11.008.

Wain, D.J., J. Lilly, A.H. Callaghan, I. Yashayaev, and B. Ward. 2015. A breaking internal wave in the surface ocean boundary layer. *Journal of Geophysical Research* 120:4,151–4,161, https://doi.org/10.1002/2014JC010416.

Walesby, K., J. Vialard, P. Minnett, A.H. Callaghan, and B. Ward. 2015. Observations indicative of rain-induced double diffusion in the ocean surface boundary layer. *Geophysical Research Letters* 42:3,963–3,972, https://doi.org/10.1002/2015GL063506.

Ward, B., T. Fristedt, A.H. Callaghan, G. Sutherland, X. Sanchez, J. Vialard, and A. ten Doeschate. 2014. The Air-Sea Interaction Profiler (ASIP): An autonomous upwardly-rising profiler for microstructure measurements in the upper ocean. *Journal of Atmospheric and Oceanic Technology* 31:2,246–2,267, https://doi.org/10.1175/JTECH-D-14-00010.1.

Weber, J.E. 2001. Virtual wave stress and mean drift in spatially damped surface waves. *Journal of Geophysical Research* 106:11,653–11,657, https://doi.org/10.1029/1999JC000035.

Weber, J.E.H., G. Broström, and Ø. Saetra. 2006. Eulerian versus Lagrangian approaches to the wave-induced transport in the upper ocean. *Journal of Physical Oceanography* 36:2,106–2,118, https://doi.org/10.1175/JPO2951.1.

Wilkin, J., L. Rosenfeld, A. Allen, R. Baltes, A. Baptista, R. He, P. Hogan, A. Kurapov, A. Mehra, J. Quintrell, and others. 2017. Advancing coastal ocean modelling, analysis, and prediction for the US Integrated Ocean Observing System. *Journal of Operational Oceanography* 10:115–126, https://doi.org/10.1080/1755876X.2017.1322026.

ACKNOWLEDGMENTS

Financial support from the Research Council of Norway through grants 244262 (RETROSPECT) and 237906 (CIRFA) is gratefully acknowledged. ØB gratefully acknowledges support from Copernicus Marine Environment Monitoring Services and Mercator International through the Service Evolution project WaveFlow. BW acknowledges funding for this research provided by Science Foundation Ireland, award 16/TIDA/3916, and the Irish Marine Institute under grants PBA/ME/16/01 and INF/17/003.

AUTHORS

Kai H. Christensen (kaihc@met.no) is Head of Division for Ocean and Ice, Norwegian Meteorological Institute, and Associate Professor, University of Oslo, Oslo, Norway. **Øyvind Breivik** is Head of Division for Oceanography and Marine Meteorology, Norwegian Meteorological Institute, Oslo, Norway, and Professor, University of Bergen, Bergen, Norway. **Knut-Frode Dagestad** is Scientist, and **Johannes Röhrs** is Scientist, both at the Norwegian Meteorological Institute, Oslo, Norway. **Brian Ward** is Scientist, National University of Ireland, Galway, Ireland.

ARTICLE CITATION

Christensen, K.H., Ø. Breivik, K.-F. Dagestad, J. Röhrs, and B. Ward. 2018. Short-term predictions of oceanic drift. *Oceanography* 31(3):59–67, https://doi.org/10.5670/oceanog.2018.310.